INFLUENCE OF PROCESSES ON THE SUN AND IN THE INTERPLANETARY MEDIUM ON THE SOLAR PROTON EVENT ON MARCH 30, 2022

© 2025 N. A. Vlasova[a,*], G. A. Bazilevskaya[b], E. A. Ginzburg[c], E. I. Daibog[b], V. V. Kalegaev[a,d], K. B. Kaportseva[a,d], Yu. I. Logachev[a], I. N. Myagkova[a]

[a]*Skobeltsyn Institute of Nuclear Physics, Moscow State University, Moscow, Russia*

[b]*Lebedev Physical Institute, Russian Academy of Sciences, Moscow, Russia*

[c]*Fedorov Institute of Applied Geophysics, Moscow, Russia*

[d]*Faculty of Physics of Lomonosov Moscow State University, Moscow, Russia*

**e-mail: nav19iv@gmail.com*

Received March 02, 2024

Revised April 01, 2024

Accepted July 25, 2024

Abstract. The results of a comparative analysis of the solar proton event on March 30, 2022, which has an unusual time profile of solar proton fluxes, with the previous and subsequent solar proton events (March 28, 2022 and April 02, 2022) are presented. Increases in energetic proton fluxes in interplanetary and near-Earth space are associated with successive solar X-ray flares M4.0, X1.3 and M3.9 and three halo-type coronal mass ejections. The work was done based on experimental data obtained from spacecraft located in interplanetary space (ACE, WIND, STEREO A, DSCOVR), in a circular polar orbit at an altitude of 850 km (Meteor-M2) and in geostationary orbit (GOES-16, Electro-L2). An explanation has been proposed for the features of the energetic proton flux profile in the solar proton event on March 30, 2022: protons accelerated in the flare on March 30, 2022 were partially screened by an interplanetary coronal mass ejection, the source of which was the explosive processes on the Sun on March 28, 2022; late registration of maximum proton fluxes, simultaneous for particles of different energies, is due to the arrival of particle fluxes inside an interplanetary coronal mass ejection. The spatial distribution of solar protons in near-Earth orbit was similar to the distribution at the Lagrange point *L1,* but with a delay of ~50 min.

Keywords: *solar proton event, solar flare, coronal mass ejection, solar wind, interplanetary magnetic field*

DOI: 10.31857/S00167940250602e6

1. INTRODUCTION

Solar proton events (SPEs) recorded in near-Earth space are the result of many physical processes occurring in the solar corona, in the interplanetary medium, and even in the Earth's magnetosphere. Statistical regularities, typical and extreme characteristics of PCA can be determined with the help of PCA catalogs, which contain many years of homogeneous series of experimental data (e.g., [Logachev et al., 2022]). But only the results of a particular event study paint a true picture of the phenomena occurring on the Sun and in the interplanetary medium. Despite many years of research, there is no unambiguous solution to the question of even the source of energetic solar particles. After the discovery of solar cosmic rays, flares were considered to be their source [Meyer et al., 1956]. The results of studies of coronal mass ejections (CMEs) led to the realization that particle acceleration is also possible in the shock waves that precede CMEs [Kahler et al., 1984; Reames, 1995]. Solar energetic particles are now assumed to be accelerated both in the solar flare region and on shock waves associated with the CME (e.g., [Reames, 2013, 2017; Bazilevskaya, 2017; Klein and Dalla, 2017]). Acceleration on shock waves accompanying a CME can occur both during the nucleation of a CME on the Sun and in the interplanetary medium (e.g., [Reames, 2013; Bazilevskaya et al., 2023]). At the same time, a very small number of SPSs have been observed that were associated only with a CME without a solar flare [Marqué et al., 2006]. Models of solar energetic particle propagation have been created that take into account the acceleration of particles in the solar corona and in the interplanetary medium [Frassati et al., 2022; Zhang et al., 2023].

The main factor determining the dynamical processes in the interplanetary medium is the interplanetary magnetic field [Parker, 1965]. Magnetic inhomogeneities embedded in the solar wind plasma affect the motion of solar energetic particles and cause modulation of their fluxes with characteristic times ranging from several minutes to several days. In particular, the magnetic structures of the solar wind can form particle traps, capturing them in confined regions of space.

The empirical "reflection model" assumes the trapping and transport of particles in translucent magnetic traps formed by the force lines of the interplanetary magnetic field (IMF) extended from the Sun [Lyubimov, 1988; Lyubimov and Grigorenko, 2007]. In [Dybog et al., 2017], the existence of variations in the Jupiterian electron fluxes near the Earth is explained, in particular, by electrons staying in magnetic traps, which have the form of closed magnetic structures arising from the interaction of different-speed solar wind fluxes (*Stream Interaction Region*, SIR). If different-speed streams exist for a long time, rotating together with the Sun, corotating interaction regions (CIR) arise, which can influence the dynamics of solar energetic particles (e.g., [Richardson, 2004; 2018]).

In [Reames, 2013; 2023], regions of space behind a propagating shock front containing trapped particles are described. In [Vlasova et al., 2024], the existence of a closed trap region formed by two interplanetary coronal mass ejections (ICMEs) and the interaction regions of high-speed and slow solar wind streams was proposed to explain the prolonged observation of solar energetic proton fluxes in the heliosphere.

It is known that MCWMs have an impact on the flux of solar energetic particles. According to Explorer-12 data, an increase in the flux of *energetic* particles, called *Energetic Storm Particles*, was detected before the "plasma cloud" that caused a magnetic storm on the Earth [Bryant et al., 1962]. The paper concluded that these are solar protons trapped inside the plasma cloud. The results of the study of the arrival of solar protons on the SOHO spacecraft when the spacecraft was in the magnetic cloud indicate that the magnetic field in the CME structure provides a "backbone" path for the propagation of proton fluxes [Torsti et al., 2004]. The use of solar energetic particles as a tool to study the magnetic field topology of two magnetic clouds has shown that in one case by the reflection of particles one should visualize the magnetic loop as a bottle connected to the Sun, in the second case the reflection is from the magnetic mirror formed by the compression field behind the shock, i.e. it is− the topology of open force lines [Tan et al., 2014]. It was shown in [Shen et l., 2008] that the proton flux with energies ≥10 MeV in the event November 05, 2011 was the largest in solar activity cycle 23 due to the fact that the particles were trapped in a structure consisting of a shock wave and a magnetic cloud. At the same time, for the event of July 14, 2000 (GLE 59), a two-stage rapid intensity drop is observed on the profile of proton fluxes with energies from ~ 1 to ~ 100 MeV, associated with the compression region and the magnetic cloud [Wu and Quin, 2020]. In [Cane et al., 1988], the results of a study of the effect of the shock wave preceding the CME, which is on the path of particle propagation in the interplanetary medium, on the time profiles of solar protons as a function of the heliolongitude of their source are presented. In [Kahler and Reames, 1991] it is concluded that magnetic clouds are almost transparent to solar particles (electrons with E = 0.2− 2 MeV, protons with E = 22− 27 MeV, KA ISEE-3) and magnetic cloud fields are not closed. In [Masson et al., 2012], based on the results of the study of GLE events using neutron monitor data, it is shown that the arrival time of the first high-energy particles on the Earth is largely determined by the type of the MMP in which the particles propagate. The initial arrival time corresponds to that expected in the Parker model in the slow solar wind and is much longer in heliospheric structures such as the ICWM. In [Kocharov et al., 2005], it is concluded that the magnetic trap-like structure of the MCWM significantly changes the intensity-time profile of high-energy particles observed at 1

a.u. The decline of the particle flux after the maximum is slower than in the Archimedean spiral magnetic field modeling and can be approximated by an exponential function.

The purpose of this work is to explain the reasons for the formation of a complex temporal profile of solar energetic proton fluxes March 30 − 31, 2022, different from the corresponding profiles in the previous and subsequent solar proton events March 28, 2022 and April 01, 2022, based on the results of the analysis of solar sources of energetic particles and high-speed solar wind fluxes, as well as the conditions in the interplanetary medium, in which solar protons propagated from the Sun to the Earth's orbit.

2. SOURCES OF EXPERIMENTAL DATA

The study of the time profiles of solar proton fluxes on March 28, 2022, March 30, 2022, and April 02, 2022 was performed on the basis of experimental data obtained from spacecraft (SC) located in interplanetary space and in the Earth's magnetosphere (Table 1).

TABLE 1.

STEREO A spacecraft during the period under study (March 30, 2022) was located at a distance of 0.97 a.u. from the Sun, and the region on the Sun associated with the spacecraft by the force lines magnetic field at a solar wind speed of 400 km/s is about 35.3° east than the corresponding region for the Earth [Gieseler et al., 2022; https://solar-mach.github.io/].

Electronic resources from which the information needed for the study was obtained:

- On solar flares and coronal holes (https://www.solarmonitor.org/);
- on coronal mass ejections from the LASCO/C2 coronagraph on the SOHO spacecraft (https://cdaw.gsfc.nasa.gov/CME_list/);
- the position of dimmings for determining the heliocoordinates of the CME (https://www.sidc.be/solardemon/);
- on images of the Sun at different wavelengths from SDO (https://www.spaceweatherlive.com; https://www.sidc.be/solardemon/);
- by synoptic maps of the Sun (https://gong.nso.edu/);
- on the time of arrival of the CME shock waves to near-Earth space (ECS) (https://zenodo.org/record/7991430);
- on the results of modeling the arrival of ICWM into near-Earth space of the solar wind and CME forecasting service Euler MMI SPbSU and LETI (https://solarwind.entroforce.ru/);
- on solar wind and interplanetary magnetic field with ACE and DSCOVR satellites (https://swx.sinp.msu.ru/);

- on solar energetic proton fluxes with STEREO A and WIND spacecraft (https://cdaweb.gsfc.nasa.gov/), with ACE spacecraft and GOES-16, Meteor-M2, Electro-L2 satellites (https://swx.sinp.msu.ru/).

Most of the figures of this article were created on the site of the Operational Space Monitoring Data Center (OSMC) of the Moscow State University Research Institute of Nuclear Physics, which provides access to operational data of space experiments and models of operational forecasting of space weather phenomena. The CDOCM website in the section "Space Weather" (https://swx.sinp.msu.ru/) contains data necessary for assessing and analyzing the radiation situation not only in near-Earth space but also in the interplanetary environment. Electronic interactive versions of catalogs of solar proton events of solar activity cycles 24 and 25 and links to printed versions of SPS catalogs of solar activity cycles 20-24 are also presented there (https://swx.sinp.msu.ru/apps/sep_events_cat/index.php?gcm=1&lang=ru).

Advanced graphical applications make it possible to perform comparative analysis of both experimental data and modeling results.

3. EXPERIMENTAL RESULTS

The peculiarity of the discussed solar proton event 30.03.2022 is that the temporal profiles of particle fluxes have a more complex shape compared to the profiles of the preceding (28.03.2022) and following (April 02, 2022) events (Fig. 1*b*). The SPSs of 28.03.2022, 30.03.2022, and 02.04.2022 are associated with solar flares of X-ray magnitude (Fig. 1*a*) M4.0 (W09), X1.3 (W31), and M3.9 (W68), respectively (the flare heliolongitude is indicated in parentheses). The flares of 28.03.2022 and 30.03.2022 occurred in the same active region. All three flares were accompanied by halo-type CMEs. The conditions in the interplanetary medium during the particle propagation of the three PCAs were different (Figs. 1*c*, 1*d*). Each event was accompanied by a high-velocity solar wind flow. In the last decade of March 2022, two coronal holes (CHs) passed through the central meridian of the Sun: 22− 24.03.2022– near-equatorial of rather large area; 29− 31.03.2022– mid-latitude of small area. High-speed solar wind streams, through which the Earth passed 27− 28.03.2022 and 02.04.2022 (Fig. 1*c*), could have their sources exactly these CDs, as the speed of the streams was~ 550 km/s, which corresponds to the time of propagation from the Sun to the Earth –~ 3 days. On 28.03.2022 on the Sun in the active region AO12975, located near the center of the Sun's disk, with a time difference of about 8 hours there were two flares of M4.0 and M1.0, accompanied by coronal mass ejections of the "halo" type. The first of the flares is associated with the SPE on 28.03.2022, and no additional growth of the solar proton flux was registered after the second flare. The interaction of two CMEs led to the

formation of an ICWM propagating toward the Earth. The arrival of the shock wave associated with this MCWM was recorded on 31.03.2022 at 01:44 UT at the L1 point and at 02:24 UT at the Earth's orbit (https://zenodo.org/record/7991430).

Fig. 1.

It can be seen that during the SPE on 30.03.2022, the strongest MMP was observed, as well as a prolonged large negative value of the *Bx-component of the* MMP (Fig. 1*g*). The time profiles of solar proton fluxes presented in Fig. 1*b* are constructed from measurements inside the Earth's magnetosphere on the GOES-16 satellite. A similar shape of all three profiles of energetic proton fluxes was also observed at the Lagrangian point *L1* on the ACE satellite (Fig. 2*a*), and in the region of the Earth's polar caps on open force lines of the Earth's magnetic field on the Meteor-M2 satellite in the northern and southern polar caps (Fig. 2*b*), and in the geostationary orbit on closed force lines on the Elektro-L2 satellite (Fig. 2*c*). Consequently, we can say that the peculiarities of the particle flux profiles on 30.03.2022 are not related to the penetration of particles into the Earth's magnetosphere.

Fig. 2.

For a more accurate assessment of the differences in the temporal profile of solar proton fluxes 30− 31.03.2022 from the profiles in the PCA 28.03.2022 and 02.04.2022, Fig. 3 presents on a unified scale the profiles of proton fluxes from GOES-16 satellite data during the first days after solar flares with which SPSs are associated. Several features of the profile of 30.03.2022 (Fig. *3b*) can be emphasized:

Fig. 3.

-the beginning of the flux increase of particles with energies > 5 MeV and > 10 MeV occurs earlier than the time of the flux increase of more energetic particles (E > 100 MeV), which testifies against their origin from a single source;

- the time interval between the beginning of the flare and the arrival of particles with E > 100 MeV for the PCA 30.03.2022 is 109 min, which is much longer than for the PCA 28.03.2022 (47 min) and the PCA 02.04.2022 (46 min), and does not correlate with the distance between the flare longitude and the Earth's conjunction longitude;

- The time interval between the flare onset and the observation of the maximum fluxes of protons with E >10 MeV for the 30.03.2022 SPS (~ 12.6 h) is significantly longer than for the 28.03.2022 SPS (4 h) and the 02.04.2022 SPS (3 h); the time of observation of the maximum in the SPS 28.03.2022 and 02.04.2022 depends on the proton energy, in the SPS 30.03.2022 maximum proton fluxes of different energies were observed simultaneously;

- the maximum proton flux, especially in the higher energy region, in the PCA on 30.03.2022 is significantly smaller than in the other two events, in spite of the fact that the X-ray flare score on 30.03.2022 is the highest: X1.3 compared to M4.0 and M3.9;

- the shape of the particle flux profile up to the maximum is significantly different for the 30.03.2022 event.

Fig. 4.

Fig. 4 shows the SPS on 28.03.2022 and 30.03.2022 from observations on the WIND spacecraft and on the STEREO A spacecraft, which at the end of March 2022 was at a distance of 0.97 a.u. from the Sun and 33.5° east of the Earth. Time profiles of solar proton fluxes measured at libration point *L1* on the WIND spacecraft and on the STEREO A spacecraft practically coincide on 28.03.2022. In the event of 30.03.2022, the profile according to the STEREO A spacecraft differs little from 28.03.2022, while on the WIND spacecraft at the *L1* point there is a significant difference between the profiles of 28.03.2022 and 30.03.2022.

4. DISCUSSION

The complex temporal profile of solar energetic proton fluxes on 30-31.03.2022 may be due to the peculiarities of the processes of particle generation and acceleration on the Sun and propagation in the interplanetary medium.

4.1 Conditions on the Sun

We analyzed solar sources of particle fluxes and perturbed solar wind for the time period under study using ultraviolet images of the solar disk at times presumably corresponding to the CME observation in the Sun's lower corona (https://www.spaceweatherlive.com/) and CME images in the coronagraph (https://www.sidc.be/cactus/catalog/LASCO/2_5_0/qkl/2022/03/). In addition, we studied difference images (obtained by successively subtracting frames from the first frame for each observation) at a wavelength of 21.1 nm (https://www.sidc.be/solardemon/), the so-called "coronal dimmings"– darker regions in the image due to density fluctuations in the solar corona (e.g., [Reinard and Biesecker, 2008]). Coronal dimmings can be related, among other things, to the escape of the CME from the corona. The results of the analysis show that the location of the dimmings corresponds to the location of the flares and is consistent with the direction of the CME propagation observed in the coronagraph. This suggests that the flares were indeed accompanied by the observed CMEs and the processes were localized in approximately the same region of the Sun, and also allows us to determine the temporal and spatial parameters of the CME evolution at early stages.

TABLE. 2.

Table 2 presents parameters of solar flares, coronal mass ejections, active regions (ARs) on the Sun, and calculated values derived from solar images and from the average solar wind speed during the PCA observations.

During the early evolution of the CMEs, the coronal propagation of solar protons can be affected (e.g., [Zhang et al., 2023]). We compared the characteristics of the corresponding dimmings to test whether the differences in SPS observed on 28.03.2022, 30.03.2022, and 02.04.2022 could be explained by the difference in proton propagation in the solar corona. We estimated the time difference between the flare (from X-ray data) and the onset of CME expansion (from difference images of the Sun). In the case of the PCA on 30.03.2022, this is the shortest time: 9 minutes compared to 22 and 19 minutes. The parameters of the three CMEs derived from the coronograph data differ slightly (Table 2), although the 30.03.2022 CME is less fast and its positional angle is the largest. The longitude of the region on the Sun connected with the Earth by force lines of the interplanetary magnetic field was calculated from the value of the mean solar wind speed at the time of the arrival of the first solar energetic protons in near-Earth space. The difference between the obtained longitude and the longitude of the flare corresponds to the angular distance of coronal proton propagation. It is practically the smallest for the SPS 30.03.2022. The results of the analysis presented in Table 2 show that in all three cases, the difference between the source longitude and the geoeffective longitude cannot provide the observed difference in the SPS registration time near the Earth's orbit. Also, the CME velocities determined in the coronagraph do not indicate that the event of 30.03.2022 is fundamentally different from the others. If we assume a coronal expansion velocity of ~ 1000 km/s, then the coronal propagation time from the perturbation onset point to the geoeffective longitude will be 8, 6, and 5 minutes for the three consecutive events under consideration. Thus, the peculiarities of the temporal profile of particle fluxes on 30.03.2022 were not related to particle propagation in the Sun's corona.

The analysis of synoptic maps of the Sun (https://gong.nso.edu/) showed that on 28.03.2022, the flare and the connection point with the STEREO A satellite were in the negative magnetic field region, while the connection point with the Earth (with the libration point *L1*) was in the positive field region and separated from the flare by the polarity separation line, but the characters of the temporal profiles of particle fluxes on the STEREO A satellite and at the *L1* point coincide (Fig. 4).

Fig. 4.

In the event of 30.03.2022, the relative positions of the flare, STEREO A, and the Earth changed little, while the profiles of the initial phase of proton flux enhancement from STEREO A and WIND data differ very significantly. Consequently, the polarity interface had no effect on the coronal proton

propagation in the 30.03. 2022 event. This conclusion is consistent with earlier results indicating that crossings of the heliospheric current layer do not affect the decline in the profile of solar proton fluxes with energies of 1− 5 MeV [Kecskeméty et al., 2009]. The above results of the study of conditions and processes on the Sun during the three events under consideration do not allow us to distinguish the SPE 30.03.2022 in a significant way.

4.2 Conditions in the interplanetary medium

Let us consider the possible influence of conditions in the interplanetary medium on the flux of solar protons propagating from the Sun to near-Earth space. On 28.03.2022, 2 CMEs were registered in AO 12975, and the second of them, observed ~8 h later, had a higher velocity (Table 2) and acceleration: at 20Rs (Rs is the Sun's radius), the first CME had zero velocity, and the second had 1300 km/sec. The interaction of the two CMEs led to the formation of the ICWM, whose shock wave reached the *L1* point on 31.03.2022 at 01:44 UT, and the Earth at 02:24 UT (https://zenodo.org/record/7991430).

Fig.5.

Fig. 5 presents the temporal structure of the MCWM at the *L1* point and of the proton fluxes at *L1* from data of the ACE spacecraft and at the geostationary orbit from data of the GOES-16 satellite. The vertical dashed lines correspond to the features of the temporal profile of the MCWM and solar proton fluxes. Line 1 shows the time of arrival of the shock front at point *L1*, followed by a turbulent region (the area between lines 1 and 3 in this figure) with rapid changes in the MMP components characteristic of a magnetic cloud envelope [Burlaga et al., 1981; Burlaga, 1988]. Within this region, a stronger MMP was observed between lines 1 and 2, which was accompanied by an increase in the solar proton fluxes to the maximum values according to the ACE satellite data. The MMP structures in front of line 3, corresponding to the inner part of the turbulent region, were accompanied by a small local decrease of the particle fluxes on the ACE satellite. Line 3 corresponds to the entrance to the magnetic cloud, with characteristic properties [Burlaga et al., 1981; Burlaga, 1988; Pal et al., 2020; Vörös et al., 2021]: enhanced magnetic field, slow changes in its direction (signs of field vector rotation), practical absence of MMP fluctuations, low solar wind density, and low plasma temperature (not shown in the figure). At moment 4, in our opinion, an exit from the magnetic cloud is observed, as the rate of change of the magnetic field direction decreases significantly (the *Bx*- and By-components practically cease to change). In the catalog (https://izw1.caltech.edu/ACE/ASC/DATA/level3/icmetable2.htm) only the duration of the entire MCWM is given (12:00 UT 31.03.2022 - 12:00 UT 01.04.2022).

As can be seen in Fig. 5, there is a time shift of ~ 50 min between the time profiles of proton fluxes measured on the ACE spacecraft and on the GOES-16 satellite, which is the time required for the solar wind to travel 1.5 million km at the solar wind velocity (~ 500 km/s) currently observed at point *L1* (Fig. 5*b*). The structure of the magnetic field inside the MCWM maintained a nearly constant spatial distribution of particle fluxes within it, which may imply the propagation of protons with energies at least up to 60 MeV in space along with the MCWM. This phenomenon requires further investigation. Thus, the peculiarities of the temporal profile of solar proton fluxes in the 30.03.2022 event are explained by the conditions in the interplanetary medium, in particular, by the role of the MCWM. It should be noted that this MCVM passed the STEREO A spacecraft, which did not observe any peculiarities of the temporal profile of proton fluxes.

One can try to estimate the radial size of the heliospheric structure through which the Earth passes:

- the full radial size of the MCWM (according to the catalog (https://izw1.caltech.edu/ACE/ASC/DATA/level3/icmetable2.htm) from 12:00 UT 31.03.2022 to 12:00 UT 01.04.2022) at the average solar wind speed~ 500 km/s is~ 0.3 a.u.;

- the radial size of the magnetic cloud (between dashed lines 3 and 4 in Fig. 5) is~ 0.18 a.u.

The estimate of the size of the MCWM on 31.03.2022 agrees with earlier results: 0.2÷0.4 a.u. [Lepping et al., 1990].

Fig. 6.

The analysis of the dynamics of the energy spectrum index of proton fluxes, when approximated by a steppe function, $E^{-\gamma}$ gives an opportunity to describe more accurately different parts of the complex and unusual temporal profile of the particle flux on 30.03.2022. In Fig. 6 shows the 5-min values of proton fluxes from GOES-16 satellite data and an exponent of the integral energy spectrum of solar protons in the stepped representation ($E > 5$ MeV÷ $E > 100$ MeV). To obtain the spectrum, we subtracted the background - the average proton fluxes before the studied events, in the interval from 00:00 UT 27.03.2022 to 11:35 UT 28.03.2022. The spectrum indices obtained from 5-minute data were smoothed for 13 points. The square indicates the beginning of the solar flare on 30.03.2022, vertical segments 1 and 2 - the beginning of the proton flux increase in the channels with $E > 10$ MeV and $E > 60$ MeV, segment 3 - the arrival of the shock front.

It can be seen that the beginning of the growth of low-energy particle fluxes was observed before the beginning of the growth of high-energy particles. These particles, most likely from the previous increase, were accelerated by the approaching shock front, which at the time of the outburst on 30.03.2022 was at a distance of ~0.2 a.u. from the Earth. This front also caused a delay in the

arrival of the first particles from the flare on 30.03.2022 at 17:21 UT. With the arrival of more energetic particles from the 30.03.2022 flare at ~19:05 UT, the spectrum becomes tighter, γ decreasing rapidly. The flux profiles of particles with E > 60 MeV and E >100 MeV before the shock indicate their diffusive propagation. The increase in γ after the shock is due to the arrival of particles inside the ICWM. From ~06 UT 31.03.2022 to the beginning of 01.04.2022, a nearly exponential decline of the proton flux is observed with a characteristic time of ~8 h. The spectrum index γ smoothly increases. This can be interpreted as convective transport of particles in the expanding heliospheric structure and experiencing adiabatic cooling [Owens, 1979; Dybog et al., 2004; Kecskeméty et al., 2009].

The results presented in this paper are not the first to observe the effect of the MCWM on the solar energetic particle flux, but earlier results were quite inconsistent (see Introduction). The time profiles of solar particles both presented and in [Cane et al., 1988] and in a more recent book [Reames, 2017] do not resemble the solar proton flux profile of the 30.03.2022 -01.04.2022 yr. The reflective model of particle accumulation, transport, and propagation assumes the existence of magnetic structures containing translucent barriers/mirrors [Lyubimov & Grigorenko, 2007]. In the event of 30.03.2022 in Fig. 5*g* we can see the accumulation of particles behind the barrier (moment 3), which is formed by a strong magnetic field and a region with increased solar wind density and velocity (Fig. 5 *b*– *c*).

The papers [Reames, 2013; 2023] discuss in detail "reservoirs", which are large regions of space behind the propagating shock front containing trapped particles. A reservoir is located between the shock front and the Sun. According to [Reames, 2023], particle trapping in the reservoir is the result of the interaction of particles accelerated at the shock front with the Alvenovian and/or hydromagnetic wave activity accompanying the shock front. Within the reservoir, the particle fluxes are homogeneous and the dimensions of the reservoir may be several astronomical units in radius and several tens of degrees in longitude. The boundaries of the reservoir may partially coincide with the boundaries of the magnetic cloud. The heliospheric structure of 31.03.2022 can also be considered as a reservoir into which the particles already accelerated during the explosive process on the Sun on 30.03.2022 fall. The particles propagate in the interplanetary medium from the Sun to the Earth inside the ICWM. Thus, it can be stated that there is a rather large variety of approaches to explain the participation of IMWM structures and associated shock waves in the formation of the observed profiles of PCA protons.

5. CONCLUSION

Based on the results of a comparative analysis of the solar proton event on 30.03.2022 (X1.3), which has a complex temporal profile of solar proton fluxes, with the previous and subsequent solar proton events: 28.03.2022 (M4.0) and 02.04.2022 (M3.9), a scenario for the development of the SPE 30.03.2022 in near-Earth space is proposed:

- On 28.03.2022, two CMEs arise as a result of explosive processes on the Sun. The later but faster CME catches up with the earlier one, and an ICWM is formed.
- At the moment of the beginning of the solar flare at 17:21 UT on 30.03.2022, the shock front of the ICWM was at a distance of ~ 0.2 a.u. from the Earth.
- The solar event on 30.03.2022 begins at 17:21 UT, in the same active region from which the two CMEs emerged, and in a few minutes the protons overtake the MCWM, the magnitude of the magnetic field in which reaches ~ 20 nTL.

The MCWM prevents the propagation of solar protons to the Earth.

- The spatial distribution of proton fluxes inside the ICWM was similar at the *L1* point and on the Earth, but with a time lag of ~50 min.
- The magnetic field structure inside the ICWM maintained a nearly constant spatial distribution of particle fluxes inside it, which may imply the propagation of protons with energies at least up to 60 MeV in space along with the ICWM.

ACKNOWLEDGEMENTS

We thank all researchers who submit their data on proton fluxes and solar wind parameters via the Internet. Experimental data are obtained at NASA's Goddard Space Flight Center: on the solar wind and interplanetary magnetic in OMNIWeb: High Resolution OMNI (http://omniweb.gsfc.nasa.gov/form/omni_min.html); on solar proton fluxes in CDAWeb: the Coordinated Data Analysis Web (https://cdaweb.gsfc.nasa.gov/). Information on solar flares and coronal mass ejections is obtained from the Coordinated Data Analysis Workshops (CDAW) (https://cdaw.gsfc.nasa.gov), SOHO LASCO CME CATALOG (https://cdaw.gsfc.nasa.gov/CME_list/). The arrival times of CME shock waves are obtained from (https://zenodo.org/record/7991430).

We thank the staff of the Solar Wind Forecast Service (Euler MMI SPbSU, LETI) (https://solarwind.entroforce.ru/), who visualized the situation in the heliosphere on 28.03.2022−03.04.2022 specifically at our request.

FUNDING

The study was carried out within the framework of the scientific program of the National Center of Physics and Mathematics (project "Nuclear and Radiation Physics").

REFERENCES

1. *Bazilevskaya G.A., Daibog E.I., Logachev Yu.I.* Isolated events of solar cosmic rays caused by the arrival of fast storm particles (ESP) // Geomagnetism and Aeronomy. V. 63. No. 4. P. 503−510. 2023 https://doi.org/10.31857/S0016794023600254
2. *Daibog E.I., Logachev Yu.I., Keiler S., Kecskemeti K.* Series of solar events with identical declines as a tool for identifying quasi-stationary states of interplanetary space // Cosmic research. V. 42. No. 4. P. 376–383. 2004
3. *Daibog E.I., Kecskemeti K., Lazutin L.L., Logachev Yu.I., Surova G.M.* 27-day periodicity of Jovian electron fluxes in the Earth's orbit // Astron. J., 2017, V. 94, No. 12, P. 1062–1070. https://doi.org/10.7868/S0004629917120027
4. *Logachev Yu.I., Bazilevskaya G.A., Vlasova N.A., E.A. Ginzburg, E.I. Daibog, V.N. Ishkov, L.L. Lazutin, M.D. Nguyen, G.M. Surova, O.S. Yakovchuk* Catalog of solar proton events of the 24th cycle of solar activity (2009−2019). Moscow: MCD, 970 p. 2022. https://doi.org/10.2205/ESDB-SAD-008
5. *Lyubimov G.P.* Reflective model of SCR motion in loop traps // Astron. USSR Academy of Sciences circular. No. 1531. pp. 19−20. 1988
6. *Lyubimov G.P., Grigorenko E.E.* On the reflective model of solar cosmic rays // Cosmic research. V. 45. No. 1. P. 12–19. 2007
7. *Parker E.N.* Dynamic processes in the interplanetary medium / Ed. L.I. Dorman. Moscow: MIR, 1965
8. *Bazilevskaya G.A.* Once again about origin of the solar cosmic rays // Journal of Physics: Conf. Series. V. 798. P. 012034. 2017. https://iopscience.iop.org/article/10.1088/1742-6596/798/1/012034/pdf
9. *Bryant D.A., Cline T.L., Desai U.D., McDonald F.B.* Explorer 12 observations of solar cosmic rays and energetic storm particles after the solar flare of September 28, 1961 // J. Geophys. Res. V. 67. N 13. P. 4983–5000. 1962. https://doi.org/10.1029/JZ067i013p04983
10. *Burlaga L., Sittler E., Mariani F., Schwenn R.* Magnetic Loop Behind an Interplanetary Shock: Voyager, Helios, and IMP 8 Observations // J. Geophys. Res. V. 86. N A8. P. 6673–6684. 1981. https://doi.org/10.1029/JA086iA08p06673

11. *Burlaga L.F.* Magnetic clouds and force-free fields with constant alpha // J. Geophys. Res., Space Physics. V. 93. N A7. P. 7217−7224. 1988. https://doi.org/10.1029/JA093iA07p07217
12. *Cane H.V., Reames D.V., von Rosenvinge T.T.* The role of interplanetary shocks in the longitude distribution of solar energetic particles // J. Geophys. Res. V. 93. N A9. P. 9555−9567. 1988. https://doi.org/10.1029/JA093iA09p09555
13. *Frassati F., Laurenza M., Bemporad A., West M.J., Mancuso S., Susino R., Alberti T., Romano P.* Acceleration of Solar Energetic Particles through CME-driven Shock and Streamer Interaction // Astrophysical Journal. V. 926. N 2. P. 227−246. 2022. https://doi.org/10.3847/1538-4357/ac460e
14. *Gieseler J., Dresing N., Palmroos C. et al.* Solar-MACH: An open-source tool to analyze solar magnetic connection configurations // Front. Astronomy Space Sci. V. 9. 2022. https://www.frontiersin.org/journals/astronomy-and-space-sciences/articles/10.3389/fspas.2022.1058810/full
15. *Kahler, S.W., Sheeley Jr., N.R., Howard, R.A., Koomen, M.J., Michels, D.J., McGuire, R.E., von Rosenvinge, T.T., Reames, D.V.* Associations between coronal mass ejections and solar energetic proton events // J. Geophys. Res. V. 89. N A11. P. 9683−9693. 1984. https://doi.org/10.1029/JA089iA11p09683
16. *Kahler S.W., Reames D.V.* Probing the Magnetic Topologies of Magnetic Clouds by Means of Solar Energetic Particles // J. Geophys. Res. V. 96, N. A6. P. 9419−9424. 1991. https://doi.org/10.1029/91JA00659
17. *Kecskeméty K., Daibog E.I., Logachev Y.I., Kóta J.* The decay phase of solar energetic particle events // J. Geophys. Res. V. 114. N A6. 2009. https://agupubs.onlinelibrary.wiley.com/doi/pdf/10.1029/2008JA013730
18. *Klein K.*-L., *Dalla S.* Acceleration and Propagation of Solar Energetic Particles // Space Sci. Rev. V. 212. P. 1107–1136. 2017. https://link.springer.com/article/10.1007/s11214-017-0382-4
19. *Kocharov L., Kovaltsov G.A., Torsti J. Huttunen-Heikinmaa K.* Modeling the solar energetic particle events in closed structures of interplanetary magnetic field // J. Geophys. Res. V. 110. N A12. 2005. https://doi.org/10.1029/2005JA011082
20. *Lepping R.*P., *Jones J.A., Burlaga L.F.* Magnetic Field Structure of Interplanetary Magnetic Clouds at 1 AU // J. Geophys. Res. V. 95. N A8. P. 11957−11965. 1990. https://doi.org/10.1029/JA095iA08p11957
21. *Marqué C., Posner A., Klein K.L.* Solar energetic particles and radio-silent fast coronal mass ejections // Astrophys. J. V. 642. P. 1222–1235. 2006. https://iopscience.iop.org/article/10.1086/501157

22. *Masson S., Démoulin P., Dasso S., Klein K.-L.* The interplanetary magnetic structure that guides solar relativistic particles // Astron. Astrophys. V. 538. N A32. 2012. https://doi.org/10.1051/0004-6361/201118145

23. *Meyer P., Parker E.N., Simson J.A.* Solar Cosmic Rays of February, 1956 and Their Propagation through Interplanetary Space // Phys. Rev. V. 104. N 3. P. 768-783. 1956. https://journals.aps.org/pr/pdf/10.1103/PhysRev.104.768?casa_token=_yHvEAClLcEAAAAA%3AN2b4irIb6lbxj2NRvyjazm_9GMXbDKcHv9Y_ecZcJZzI_q0ZDfqSlQOwNxV7QCcsWNn_7OfaXp2VqmgB

24. *Owens A. J.* Interplanetary diffusion of solar cosmic rays—A new approximate analytic solution // J. Geophys. Res. V. 84. N A8. P. 4451 – 4456. 1979. https://doi.org/10.1029/JA084iA08p04451

25. *Pal S., Dash S., Nandy D.* Flux erosion of magnetic clouds by reconnection with the Sun's open flux // Geophys. Res. Lett. V. 47. N 8. e2019GL086372. 2020. https://doi.org/10.1029/2019GL086372

26. *Reames D.V.* Solar energetic particles: A paradigm shift // Rev. Geophys. V. 33. S1. P. 585−589. 1995. https://doi.org/10.1029/95RG00188

27. *Reames D.V.* The two sources of solar energetic particles // Space Science Reviews. 2013. V. 175. P. 53–92. https://doi.org/10.1007/s11214-013-9958-9

28. *Reames D.V.* Solar Energetic Particles. A Modern Primer on Understanding Sources, Acceleration and Propagation / Part of the book series: Lecture Notes in Physics (LNP, volume 932) 2017

29. *Reames D.V.* How Do Shock Waves Define the Space-Time Structure of Gradual Solar Energetic Particle Events? // Space Science Reviews. 2023. V. 219. A14. https://doi.org/10.1007/s11214-023-00959-x

30. *Reinard A.A., Biesecker D.A.* Coronal mass ejection associated coronal dimmings // Astrophys. J. V. 674. P. 576−585. 2008. https://iopscience.iop.org/article/10.1086/525269

31. *Richardson I.G.* Energetic particles and corotating interaction regions in the solar wind // Space Science Reviews. V. 111. P. 267–376. 2004. https://doi.org/10.1023/B:SPAC.0000032689.52830.3e

32. *Richardson I.G.* Solar wind stream interaction regions throughout the heliosphere // Living Reviews in Solar Phys. V. 15. A1. 2018. https://doi.org/10.1007/s41116-017-0011-z

33. *Shen C., Wang Y., Ye P., Wang S.* Enhancement of Solar Energetic Particles During a Shock – Magnetic Cloud Interacting Complex Structure // Solar Phys. V. 252. P. 409–418. 2008. https://link.springer.com/article/10.1007/s11207-008-9268-7

34. *Tan L.C., Malandraki O.E., Reames D.V., Ng C.K., Wang L., Dorrian G.* Use of incident and reflected solar particle beams to trace the topology of magnetic clouds // Astrophys. J. V. 750. N 2. P. 146−167. 2012. https://iopscience.iop.org/article/10.1088/0004-637X/750/2/146/meta

35. *Torsti J., Riihonen E., Kocharov L.* The 1998 may 2–3 magnetic cloud: an interplanetary "highway" for solar energetic particles observed with SOHO/ERNE // Astrophys. J. V. 600. P. L83–L86. 2004. https://iopscience.iop.org/article/10.1086/381575

36. *Vlasova N.A., Bazilevskaya G.A., Ginzburg E.A., Daibog E.I., Kalegaev V.V., Kaportseva K.B., Logachev Yu I., Myagkova I.N.* Solar Energetic Proton Fluxes in Near-Earth Space on March 13–23, 2023 // Cosmic Res. V. 62. N 2. C. 197−209. 2024. https://link.springer.com/article/10.1134/S0010952523600282

37. *Vörös Z., Varsani, A., Yordanova, E., Sasunov, Y. L., Roberts, O. W., Kis, Á., Nakamura R., Narita Y.* Magnetic reconnection within the boundary layer of a magnetic cloud in the solar wind // Journal of Geophysical Research: Space Physics. V. 126. N 9. e2021JA029415. 2021. https://doi.org/10.1029/2021JA029415

38. *Wu S.-S., Qin G.* Magnetic Cloud and Sheath in the Ground-level Enhancement Event of 2000 July 14. I. Effects on the Solar Energetic Particles // Astrophys. J. V. 904. N 2. P. 151−159. 2020. https://doi.org/10.3847/1538-4357/abc0f2

39. *Zhang M., Cheng L., Zhang J., Riley P., Kwon R.Y., Lario D., Balmaceda L., Pogorelov N.V.* A Data-driven, Physics-based Transport Model of Solar Energetic Particles Accelerated by Coronal Mass Ejection Shocks Propagating through the Solar Coronal and Heliospheric Magnetic Fields // Astrophys. J.: Supplement Series. V. 266. N 2. P. 35−54. 2023. https://doi.org/10.3847/1538-4365/accb8e

Table 1. Sources of information on solar energetic proton fluxes and parameters of the solar wind and interplanetary magnetic field

SPACECRAFT	**Orbit**	**Proton energy, MeV**
STEREO A	Heliocentric orbit, close to the Earth's orbit;	40− 60
ACE	*L1* libration point – 1.5 million km from Earth to the Sun	>10 >30
WIND	*L1* libration point – 1.5 million km from Earth to the Sun	28− 72
DSCOVR	*L1* libration point– 1.5 million km from the Earth to the Sun	–
Meteor-M2	Circular, sun-synchronous, morning Inclination 98.8° , orbital period 101.4 min.	10− 160
GOES-16	Geostationary orbit: altitude ~ 36000 km; inclination ~ 0° ; longitude – 75.2° W	> 5 > 10 > 30 > 60 > 100 > 500
Electro-L2	Geostationary orbit: altitude~ 36000 km; inclination ~ 0° ; longitude – 14.5° W	9− 20 20− 40

Table 2. Parameters of solar flares, coronal mass ejections, active regions (ARs) on the Sun and calculated values

Flares: date, onset time (UT)	**28.03.2022 г. 10:58**	**28.03.2022 г. 19:08**	**30.03.2022 г. 17:21**	**02.04.2022 г. 12:56**
Flare coordinates, ballpark, AO	N12W09 M4.0 12975	N14W07 M1.0 12975	N13W31 X1.3 12975	N12W68 M3.9 12976
CWM data *	N14W04 11:20 22 min.	N14W12	N13W32 17:30 9 min	N15W69 13:15 19 min
KVM: time of appearance in the coronograph field of view (UT)	12:00	20:24	18:00	13:36
KVM: velocity and solution parameters**	702 km/s 360° 127°	905 km/s 360° 299°	641 km/s 360° 298°	1433 km/s 360° 263°
Vsw Wφ Δφ***	520 km/s W43 34°	– – –	400 km/s W58 27°	550 km/s W42 -26°
KWM: Co	1000 km/s 8 min	– –	1000 km/s 6 min	1000 km/s 5 min
Arrival time of protons with *E*> 100 MeV (UT), ΔT from the flare	11:45 47 min	– –	19:10 109 min	13:40 46 min

*Note:** Coordinates of the CME (dimmings), time of the beginning of the CME expansion in the Sun's corona (UT) and ΔT from the beginning of the flare to the CME expansion.

** Coronograph velocity of the CME, angular solution (angular width) of the CME near the Sun, position angle of the fastest segment of the leading edge of the CME - MPA (*measurement position angle*).

*** Solar wind and associated longitude of the power line from the Earth (Wφ) and Δφ between it and the flare longitude.

Figure captions

Fig. 1. Time profiles on 27.03.2022− 05.04.2022: (*a*)− of the solar X-ray flux density with a wavelength of 0.1− 0.8 nm and (*b*)− solar proton fluxes from GOES-16 satellite data, (*c*)− solar wind velocity and density, and (*d*)− module and *Bx* -component of the MMP (*d*)− from DSCOVR satellite data.

Fig. 2. Time profiles of solar proton fluxes 27.03.2022− 05.04.2022: (*a*)− with E > 10 MeV and E > 30 MeV from ACE satellite data; (*b*)− with E= 10-160 MeV from Meteor-M2 satellite data; *(c*)− with E = 9− 20 MeV and E = 20− 40 MeV from Elektro-L2 satellite data.

Fig. 3. Time profiles of proton fluxes from GOES-16 satellite data: (*a*)− from 11:00 UT 28.03.2022 to 11:00 UT 29.03.2022, (*b*)− from 17:00 UT 30.03.2022 to 17:00 UT 31.03.2022, (*c*)− from 13:00 UT 02.04.2022 to 13:00 UT 03.04.2022.

Fig. 4. (*a*)− Time profiles of proton fluxes with E=28− 72 MeV according to WIND spacecraft and with *E* = 40− 60 MeV of STEREO A spacecraft from 27.03.2022 to 01.04.2022 (*b*)− Location scheme of STEREO A spacecraft and the Earth on 30.03.2022 (https://solar-mach.github.io/).

Fig. 5. Time profiles from 16:00 UT on 30.03.2022 to 14:00 UT on 01.04.2022.(*a)*− solar wind speed and density from DSCOVR data; (*b*)− module *B* and *Bx* and (*c*)− *By*- and Bz-components of the MMP from DSCOVR data; solar proton fluxes with energies >10 and >30 MeV from (*d*)− ACE data and (*e*) GOES-16 satellite.

Fig. 6. Time profiles of the index of the stepped energy spectrum of proton fluxes (upper curve) and proton fluxes with E > 10, 60 and 100 MeV from GOES-16 30− 31.03.2022 data: *1* - beginning of proton flux increase >10 MeV, *2* − >60 MeV, *3* - arrival of the shock front.

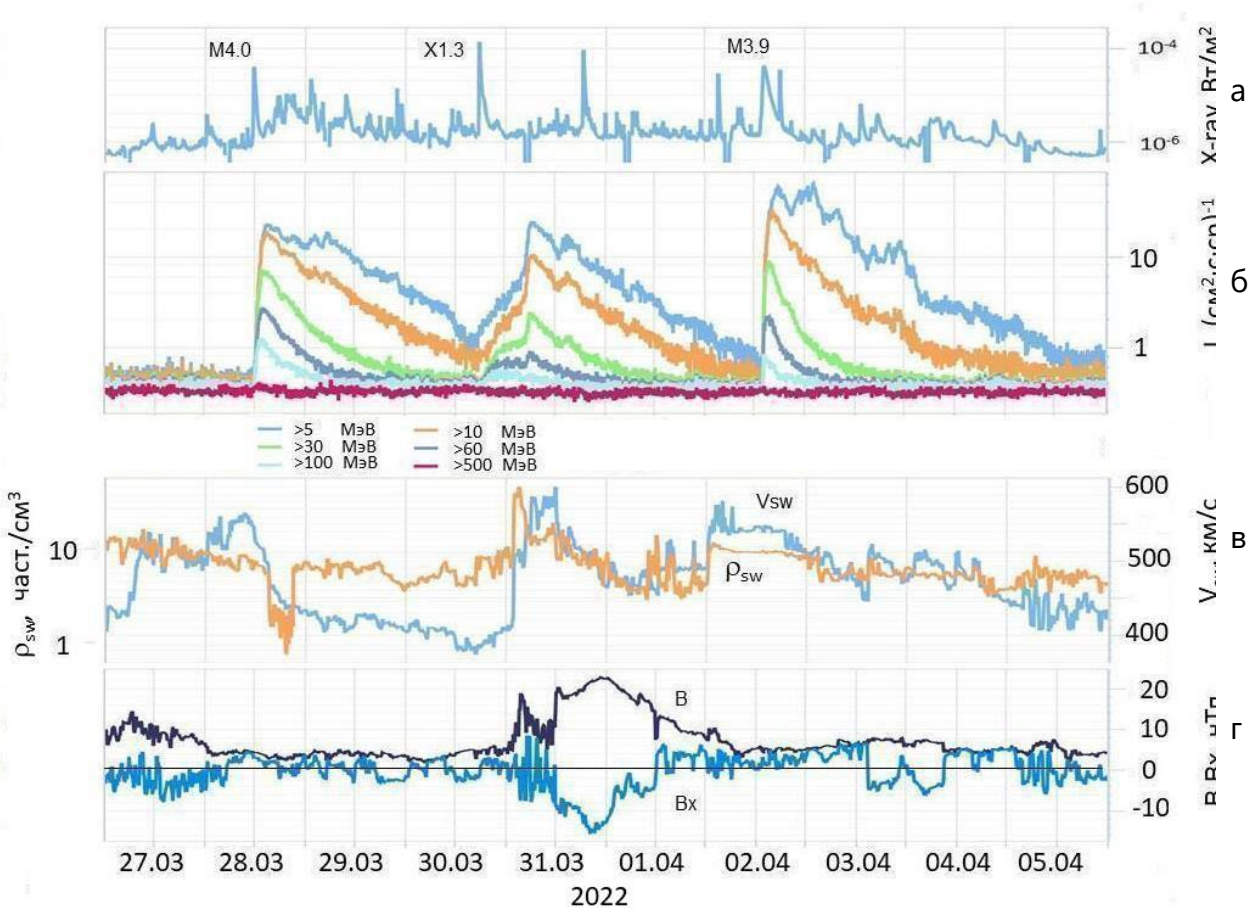
M4.0
X1.3
M3.9
10⁻⁴
10⁻⁶
а
10
1
б
>5 МэВ
>30 МэВ
>100 МэВ
>10 МэВ
>60 МэВ
>500 МэВ
600
500
400
Vsw
ρsw
ρsw, част./см³
10
1
в
20
10
0
-10
B
Bx
г
27.03
28.03
29.03
30.03
31.03
01.04
02.04
03.04
04.04
05.04
2022

Fig. 1.

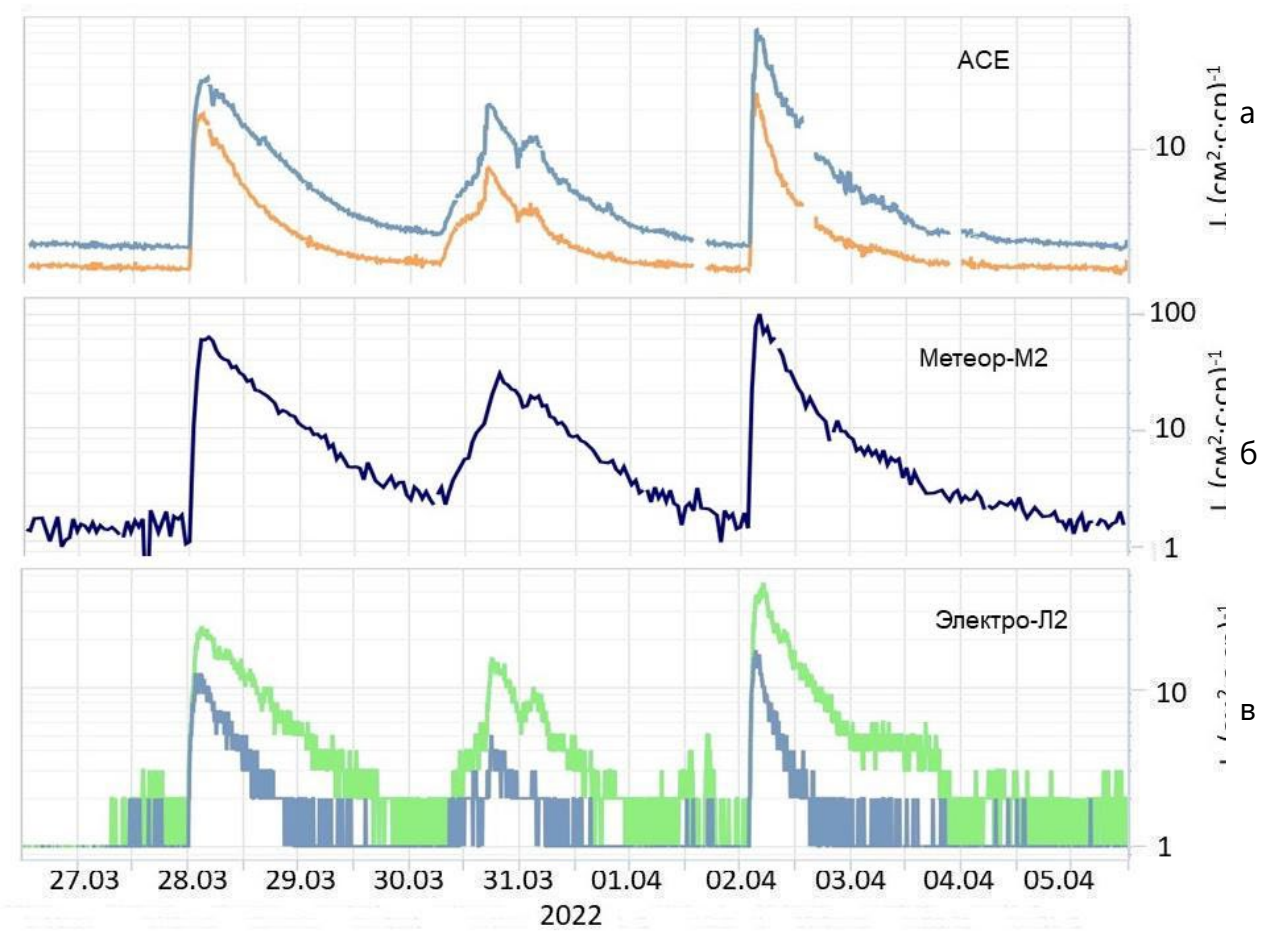
ACE
10
а
Метеор-М2
100
10
1
б
Электро-Л2
10
1
в
27.03
28.03
29.03
30.03
31.03
01.04
02.04
03.04
04.04
05.04
2022

Fig. 2.

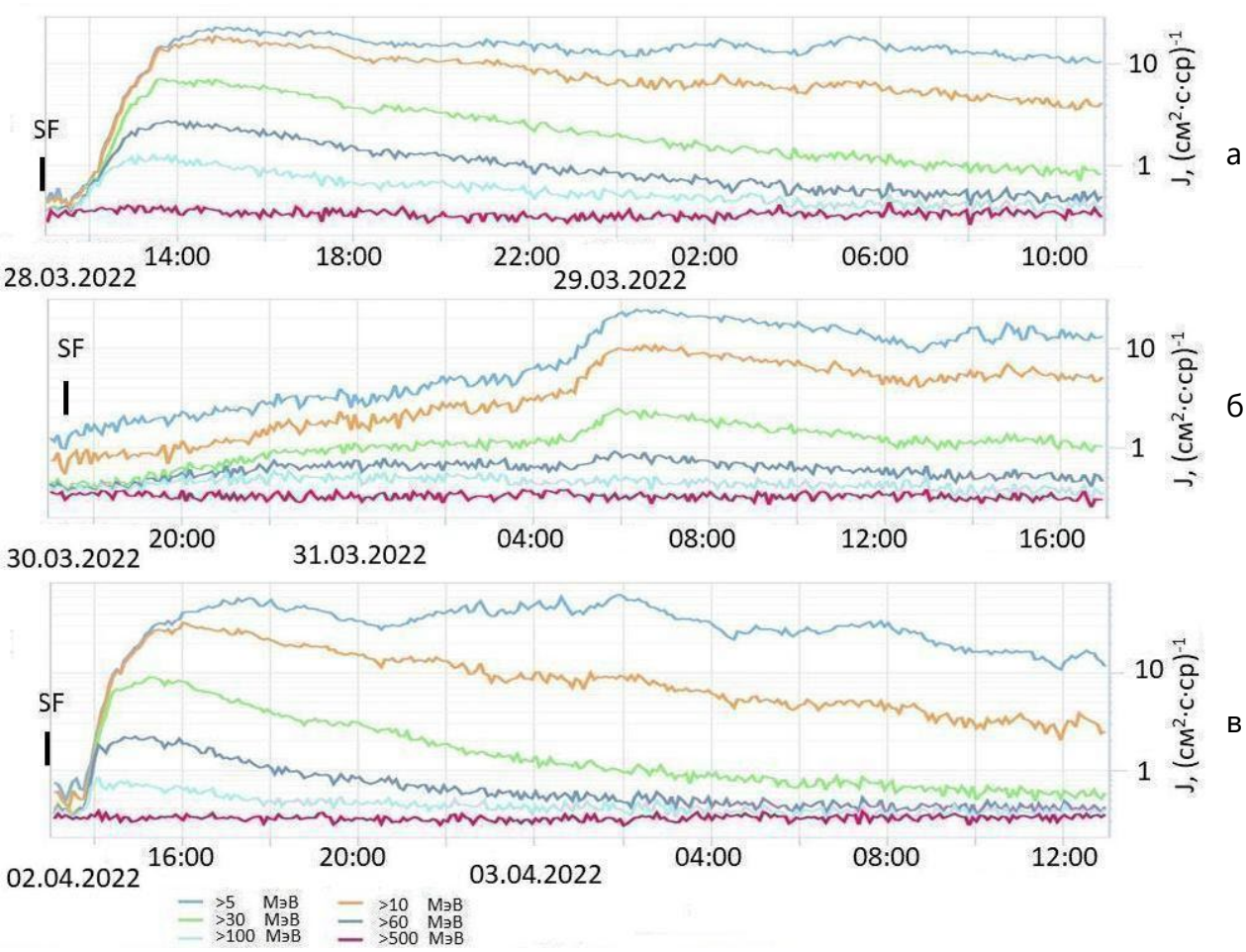
SF
10
1
J, (см²·с·ср)⁻¹
а
14:00
18:00
22:00
02:00
06:00
10:00
28.03.2022
29.03.2022
SF
10
1
J, (см²·с·ср)⁻¹
б
20:00
04:00
08:00
12:00
16:00
30.03.2022
31.03.2022
SF
10
1
J, (см²·с·ср)⁻¹
в
16:00
20:00
04:00
08:00
12:00
02.04.2022
03.04.2022
>5 МэВ
>30 МэВ
>100 МэВ
>10 МэВ
>60 МэВ
>500 МэВ

Fig. 3.

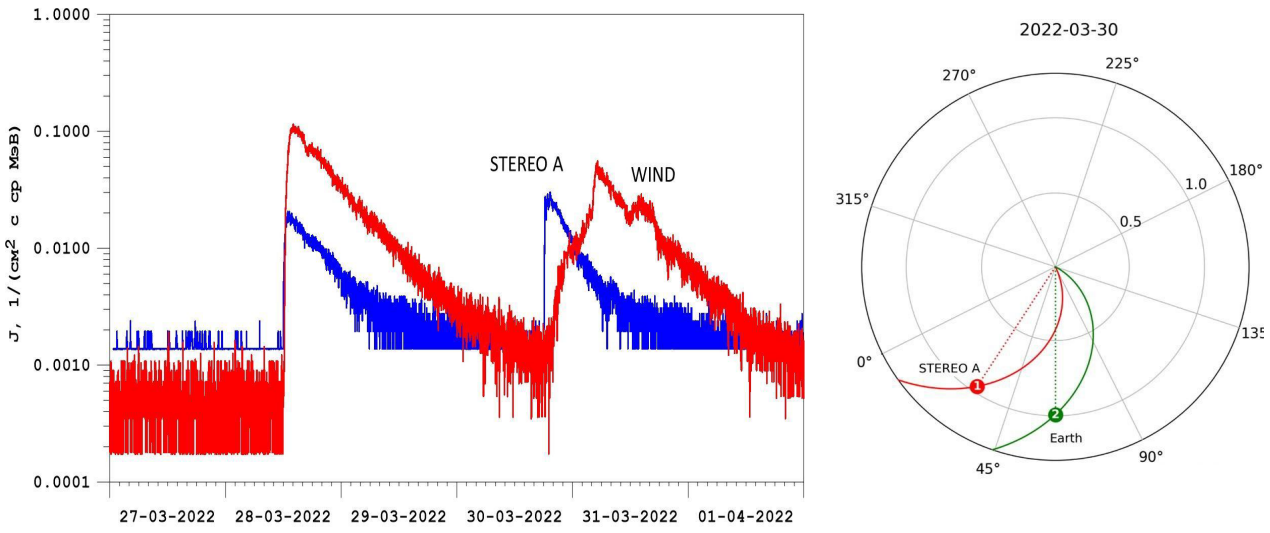
1.0000
0.1000
0.0100
0.0010
0.0001
J, 1/(см2 с ср МэВ)
STEREO A
WIND
27-03-2022
28-03-2022
29-03-2022
30-03-2022
31-03-2022
01-04-2022
2022-03-30
270°
225°
180°
315°
1.0
0.5
0°
STEREO A
Earth
45°
90°

a *b*

Fig. 4.

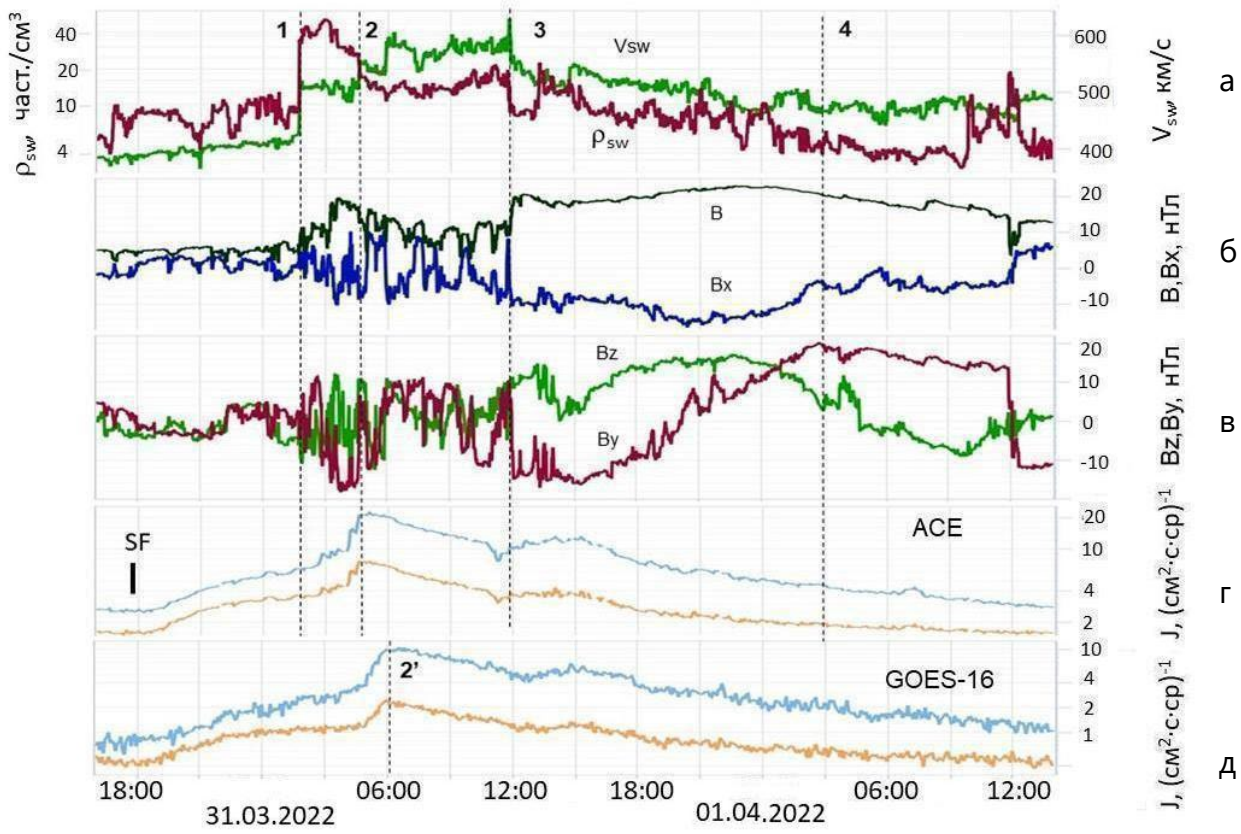
1
2
3
4
Vsw
ρsw
B
Bx
Bz
By
SF
ACE
2'
GOES-16
18:00
06:00
12:00
18:00
06:00
12:00
31.03.2022
01.04.2022
ρsw, част./см3
Vsw, км/с
B,Bx, нТл
Bz,By, нТл
J, (см2·с·ср)-1
J, (см2·с·ср)-1
а
б
в
г
д

Fig. 5.

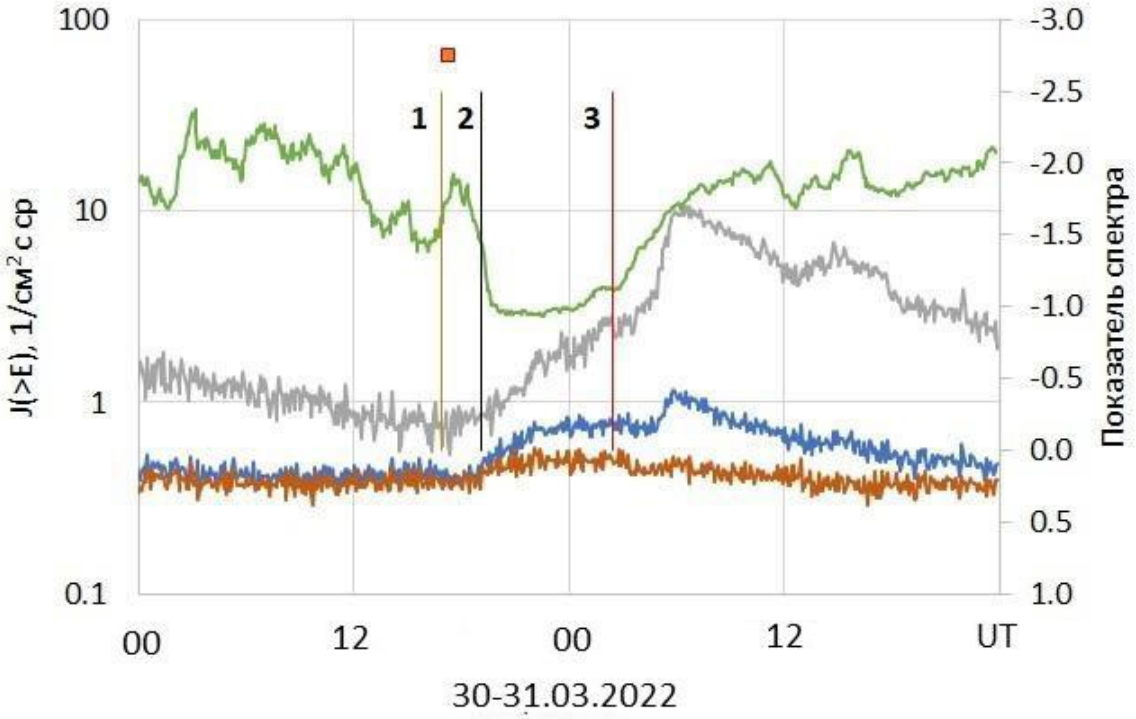
100
10
1
0.1
J(>E), 1/см² с ср
-3.0
-2.5
-2.0
-1.5
-1.0
-0.5
0.0
0.5
1.0
Показатель спектра
1
2
3
00
12
00
12
UT
30-31.03.2022

Fig. 6.